EXFOLIATED, NITROGEN-DOPED GRAPHENE NANOSHEET CATHODE FOR LITHIUM-OXYGEN BATTERIES (POSTPRINT)

Padmakar Kichambare and Stanley Rodrigues

Electrical Systems Branch
Power and Control Division

JUNE 2014

AIR FORCE RESEARCH LABORATORY
AEROSPACE SYSTEMS DIRECTORATE
WRIGHT-PATTERSON AIR FORCE BASE, OH 45433-7541
AIR FORCE MATERIEL COMMAND
UNITED STATES AIR FORCE

NOTICE AND SIGNATURE PAGE

This report was cleared for public release by the USAF 88th Air Base Wing (88 ABW) Public Affairs Office (PAO) and is available to the general public, including foreign nationals.

Copies may be obtained from the Defense Technical Information Center (DTIC) (http://www.dtic.mil).

AFRL-RQ-WP-TP-2015-0056 HAS BEEN REVIEWED AND IS APPROVED FOR PUBLICATION IN ACCORDANCE WITH ASSIGNED DISTRIBUTION STATEMENT.

*//Signature//
STANLEY J. RODRIGUES
Project Manager
Electrical Systems Branch
Power and Control Division

//Signature//
GREGORY L. FRONISTA, Chief
Electrical Systems Branch
Power and Control Division
Aerospace Systems Directorate

//Signature//
DANIEL B. THOMPSON
Acting Division Chief
Power and Control Division
Aerospace Systems Directorate

REPORT DOCUMENTATION PAGE

Form Approved
OMB No. 0704-0188

The public reporting burden for this collection of information is estimated to average 1 hour per response, including the time for reviewing instructions, searching existing data sources, searching existing data sources, gathering and maintaining the data needed, and completing and reviewing the collection of information. Send comments regarding this burden estimate or any other aspect of this collection of information, including suggestions for reducing this burden, to Department of Defense, Washington Headquarters Services, Directorate for Information Operations and Reports (0704-0188), 1215 Jefferson Davis Highway, Suite 1204, Arlington, VA 22202-4302. Respondents should be aware that notwithstanding any other provision of law, no person shall be subject to any penalty for failing to comply with a collection of information if it does not display a currently valid OMB control number. **PLEASE DO NOT RETURN YOUR FORM TO THE ABOVE ADDRESS.**

1. REPORT DATE *(DD-MM-YY)*	2. REPORT TYPE	3. DATES COVERED *(From - To)*
June 2014	Conference Proceedings Postprint	01 June 2014 – 01 June 2014

4. TITLE AND SUBTITLE
EXFOLIATED, NITROGEN-DOPED GRAPHENE NANOSHEET CATHODE FOR LITHIUM-OXYGEN BATTERIES (POSTPRINT)

5a. CONTRACT NUMBER
In-house

5b. GRANT NUMBER

5c. PROGRAM ELEMENT NUMBER
62203F

6. AUTHOR(S)
Padmakar Kichambare and Stanley Rodrigues (AFRL/RQQE)

5d. PROJECT NUMBER
3145

5e. TASK NUMBER
N/A

5f. WORK UNIT NUMBER
Q10H

7. PERFORMING ORGANIZATION NAME(S) AND ADDRESS(ES)
Electrical Systems Branch (AFRL/RQQE)
Power and Control Division
Air Force Research Laboratory, Aerospace Systems Directorate
Wright-Patterson Air Force Base, OH 45433-7541
Air Force Materiel Command, United States Air Force

8. PERFORMING ORGANIZATION REPORT NUMBER
AFRL-RQ-WP-TP-2015-0056

9. SPONSORING/MONITORING AGENCY NAME(S) AND ADDRESS(ES)
Air Force Research Laboratory
Aerospace Systems Directorate
Wright-Patterson Air Force Base, OH 45433-7541
Air Force Materiel Command
United States Air Force

10. SPONSORING/MONITORING AGENCY ACRONYM(S)
AFRL/RQQE

11. SPONSORING/MONITORING AGENCY REPORT NUMBER(S)
AFRL-RQ-WP-TP-2015-0056

12. DISTRIBUTION/AVAILABILITY STATEMENT
Approved for public release; distribution unlimited.

13. SUPPLEMENTARY NOTES
PA Case Number: 88ABW-2014-2721; Clearance Date: 04 Jun 2014.

This conference paper was published in the conference proceedings of the 46th Power Sources Conference, held June 9 - 12, 2014 at the Orlando Wyndham Resort in Orlando, FL. © 2014 Power Sources Conference. The U.S. Government is joint author of the work and has the right to use, modify, reproduce, release, perform, display, or disclose the work.

14. ABSTRACT
Cathodes prepared using grapheme nanosheets (GNSs), nitrogen-doped graphene nanosheets (N-GNSs), exfoliated nitrogen-doped grapheme nanosheets (Ex-N-GNSs) as well as composite of Ex-NGNSs with lithium aluminum germanium phosphate (LAGP) have been explored for application in lithium-oxygen batteries. These cathodes exhibit remarkable enhancement in cell capacity in comparison to conventional carbon cathodes. This enhancement is ascribed to the unique morphology of GNSs, higher oxygen reduction and oxygen evolution activity as well as fast lithium ion conduction of LAGP. These results demonstrate a strong potential of GNSs as cathodes for rechargeable lithium-oxygen batteries.

15. SUBJECT TERMS
lithium-oxygen battery, oxygen reduction reactions, nitrogen-doped carbon, lithium aluminum germanium phosphate

16. SECURITY CLASSIFICATION OF:			17. LIMITATION OF ABSTRACT:	18. NUMBER OF PAGES	19a. NAME OF RESPONSIBLE PERSON (Monitor)
a. REPORT Unclassified	**b. ABSTRACT** Unclassified	**c. THIS PAGE** Unclassified	SAR	10	Stanley J. Rodrigues **19b. TELEPHONE NUMBER** *(Include Area Code)* N/A

Standard Form 298 (Rev. 8-98)
Prescribed by ANSI Std. Z39-18

Exfoliated, Nitrogen-Doped Graphene Nanosheet Cathode
for Lithium-Oxygen Batteries

Padmakar Kichambare and Stanley Rodrigues

Air Force Research Laboratory, Aerospace Systems Directorate

Wright-Patterson Air Force Base, Ohio 45433-7252.

Abstract: *Cathodes prepared using graphene nanosheets (GNSs), nitrogen-doped graphene nanosheets (N-GNSs), exfoliated nitrogen-doped graphene nanosheets (Ex-N-GNSs) as well as composite of Ex-N-GNSs with lithium aluminum germanium phosphate (LAGP) have been explored for application in lithium-oxygen batteries. These cathodes exhibit remarkable enhancement in cell capacity in comparison to conventional carbon cathodes. This enhancement is ascribed to the unique morphology of GNSs, higher oxygen reduction and oxygen evolution activity as well as fast lithium ion conduction of LAGP. These results demonstrate a strong potential of GNSs as cathodes for rechargeable lithium-oxygen batteries.*

Keywords: Nitrogen-doped graphene nanosheets; scanning electron microscopy; oxygen reduction reaction; cyclic voltammetry; lithium-oxygen battery.

Introduction

The continuous increase in demand for energy as well as global concerns over the depletion of fossil fuels has led to the exploration of high density energy storage systems [1]. Among these energy systems, lithium-oxygen battery holds a great potential, as this battery has a theoretical energy density [2] comparable to gasoline [3]. A typical lithium-oxygen battery is composed of lithium metal anode, porous carbon based cathode exposed to gaseous oxygen, and lithium ion conducting electrolyte. During discharge, lithium is oxidized at the anode and oxygen is reduced at the cathode to produce discharge products. Subsequent charging causes the decomposition of discharge products and the generation of oxygen. Although these batteries operate on a simple chemical reaction between lithium ions and oxygen molecules, there are many technical challenges that need to be overcome for realization of practical lithium-oxygen battery operating in an ambient environment. Several factors dictate the performance of these batteries such as oxygen cathode, electrolyte composition, relative humidity, and cell design [4-7]. In particular, the material architecture of oxygen cathodes play a key role in governing the electrochemical performance of lithium-oxygen battery.

Abraham and Jiang [8] pioneered the lithium-oxygen battery technology. They reported cell capacity of 1410 mAh/g in pure oxygen atmosphere. Following this work, significant efforts have been focused on cathode formulations [9-13], efficient oxygen reduction catalysts [16-17], electrolyte compositions [14-15], effect of moisture [18], etc. In spite of these efforts to improve the sluggish kinetics of oxygen reduction reaction (ORR) as well as oxygen evolution reaction (OER) at the cathode, lithium-oxygen cells still exhibit significantly lower discharge capacity than the theoretical cell capacity, and high overpotential with limited cycle life. To this end, it is important to develop oxygen cathodes with a highly efficient ORR and OER catalyst that have significant impact on the desired energy densities of these cells. Recently, graphene nanosheets (GNSs) have been investigated as electrocatalyst for energy storage applications [19] because of its excellent electrical conductivity, distinct morphology, large surface area, and outstanding electrocatalytic activity. GNSs have been employed as oxygen cathode in fuel cells and show a higher discharge voltage under acidic condition [20]. GNSs, nitrogen-doped graphene nanosheets (N-GNSs) were also exploited in non-aqueous lithium-oxygen cells as cathode material that demonstrated an exceptionally high discharge cell capacity [21].

In continuation of our work on a fully solid-state, rechargeable lithium-oxygen cells [22-25], we report here the use of GNSs, N-GNSs, exfoliated nitrogen-doped graphene nanosheets (Ex-N-GNSs) and composite cathode prepared from mixture of Ex-N-GNSs and lithium aluminum germanium phosphate (LAGP) in a solid-state lithium-oxygen cell and compared the cell performance with cells using cathodes prepared from mesoporous carbon. Furthermore, the role of porosity, surface area and electro-catalytic activity of GNSs on the electrochemical performance is also discussed.

Experimental Details

Commercially available GNSs (Angstron Materials, Inc.) were heated in a vacuum oven at 250 °C to remove any residual surfactant. These GNSs were used for further work. N-GNSs and Ex-N-GNSs were prepared using procedure described in the literature [19]. LAGP was prepared by solid-state sintering technique.

A scanning electron microscope (SEM), (JEOL JSM-6060) equipped with energy dispersive X-ray (EDX) spectroscopy assembly was used to observe the morphologies of the specimens. Structure and purity of these materials were performed by powder X-ray diffraction (XRD) on a Bruker D8 Discover diffractometer operated at 40 kV, 40 mA current with CuKα in the 2θ range of 15 to 80° at an increment of 0.05°. The surface areas of the specimens were determined by nitrogen adsorption / desorption measurements at 77 K (Micromeritics ASAP 2020). The porosity of cathode material was characterized by a gas pycnometer (Micromeritis, Accu Pyc II 1340). Cyclic voltammetry (CV) and galvanostatic charge-discharge measurements of the specimens were conducted using a computer controlled VersaSTAT 4 (Princeton Applied Research) electrochemical workstation. CV measurements were performed in a standard three-electrode cell configuration using 0.1 M KOH as the electrolyte at 25 °C with a scan rate of 5 mV/sec. The working electrode for CV measurement was prepared by applying the paste of specimens and Nafion (tetrafluoroethylene based fluoropolymer-copolymer) on the tip of a graphite rod. A Pt wire was used as the counter electrode. All potentials were measured with respect to saturated calomel electrode (SCE).

Powders of GNSs, N-GNSs, Ex-N-GNSs, and composite **1** (mixture of Ex-N-GNSs with 5 wt % LAGP) were used to fabricate the oxygen cathode. These powders were mixed with de-ionized water and polytetrafluoroethylene (PTFE) to obtain a viscous solution. A nickel foam was then suspended in this solution with sonication for 2 hours. This process was carried to load GNSs in the open voids of nickel foam. Subsequently, the cathode specimen was dried overnight at 100 °C under vacuum. A solid-state lithium-oxygen cell with a 1 cm^2 area was fabricated using a Swagelok type cell in a dry room with controlled moisture content. Nickel foam with GNSs/N-GNSs/Ex-N-GNSs/composite **1** were used as working cathodes along with lithium metal as anode and LAGP as electrolyte.

Electrochemical impedance spectroscopy (EIS) measurements on the lithium-oxygen cells were conducted over a frequency range of 0.1 Hz to 10^6 Hz before and after discharge/charge measurements. All electrochemical tests on these cells were carried under oxygen atmosphere.
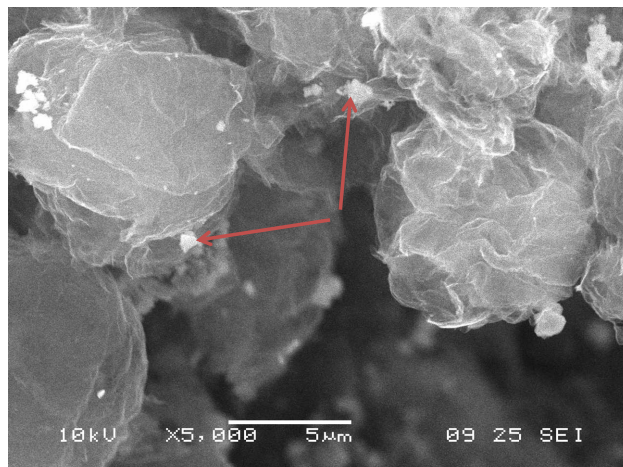

Figure 1. SEM image of composite **1** (Ex-N-GNSs and 5 wt % LAGP).

Results and Discussion

The morphology of the working cathode was examined under SEM. Figure 1 shows the SEM micrograph of composite **1** that contains wrinkled, porous, 3D architectures with interconnected pore channels of Ex-N-GNSs and crystals of LAGP (shown by arrows). This favorable morphology facilitates oxygen transport, enhances electrocatalytic activity and provides enough void to accommodate discharge products. EDX conducted on these samples revealed the nitrogen content to be 3-4 at. wt. %.

A typical nitrogen adsorption – desorption isotherm at 77 K for composite **1** is shown in Figure 2. Isotherm shows adsorption hysteresis indicating the presence of micropores The Brunauer-Emmett-Teller (BET) surface
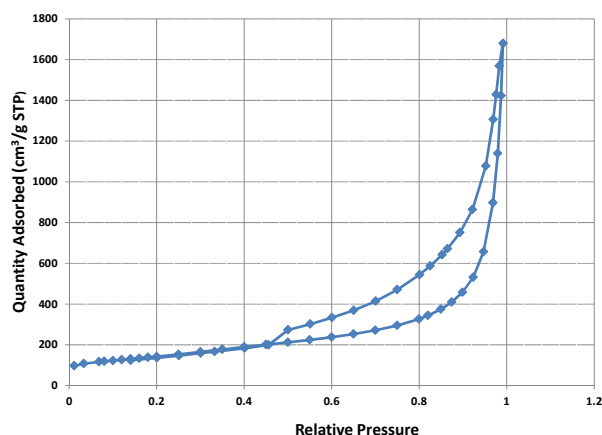

Figure 2. N$_2$ adsorption - desorption isotherm for composite **1** (Ex-N-GNSs and 5 wt % LAGP).

2
Approved for public release; distribution unlimited.

area of GNSs, N-GNSs, Ex-N-GNSs, and composite **1** were found to be 482, 583, 685, 470 m^2/g, respectively The remarkable nitrogen uptake above the relative pressure ratio of 0.40 has been observed in BET isotherm and is due to the condensation of nitrogen in mesoporous GNSs.

The CV curves recorded for GNSs, N-GNSs, Ex-N-GNSs, and composite **1** in oxygen saturated aqueous solution of 0.1 M KOH are presented in Figure 3. Well defined ORR peaks at around -0.389 V, -0.449 V, -0.397 V, and -0.478 V (vs. SCE) were observed for GNSs, N-GNSs, Ex-N-GNSs, and composite **1**, respectively, with highest reduction current density of 0.0032 A/cm^2 for composite **1.** Figure 3 also shows OER peaks at around 0.466 V, 0.496 V, 0.525 V, and 0.895 V (vs. SCE) for GNSs, N-GNSs, Ex-N-GNSs, and composite **1**, respectively. This indicates that loading of LAGP particles on Ex-N-GNSs helps improve electro-catalytic activity. No electro-catalytic activity was observed for all these cathode materials when the electrolyte was saturated with nitrogen.

Based on the high surface area, porous structure as well as electro-catalytic activity towards oxygen reduction and oxygen evolution of GNSs, N-GNSs, Ex-N-GNSs, and composite **1**, solid-state lithium-oxygen cells with 1 cm^2 active area were fabricated. The cathode side of the cell has perforations to access oxygen. The lithium anode was coupled to an oxygen cathode through a solid electrolyte laminate, described in our previous work [22]. The solid electrolyte laminate provides very high ionic conductivity for transport of lithium ions from lithium anode to oxygen cathode. In addition, the electrolyte laminate improves lithium-electrolyte interfacial stability and passivates the lithium surface.
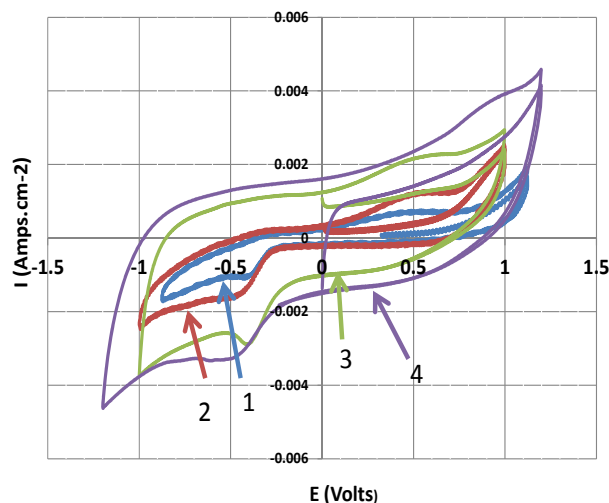

Figure 3. CV of (1) GNSs, (2) N-GNSs, (3) Ex-N-GNSs) and (4) composite **1** in oxygen saturated 0.1 M KOH at a scan rate of 5 mV/sec at 25 ^{o}C.
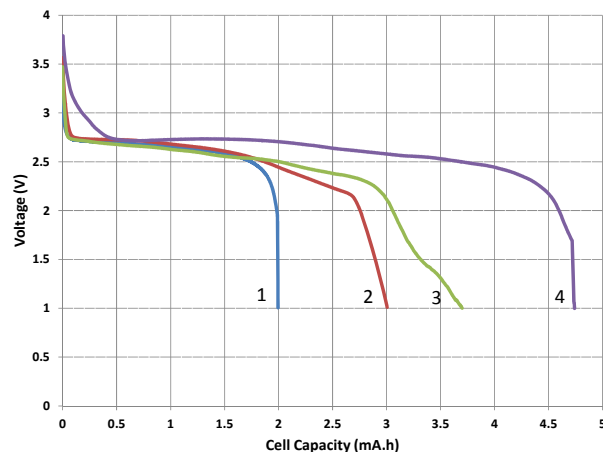

Figure 4. Discharge profiles for a lithium-oxygen cell at 75 °C using (1) GNSs, (2) N-GNSs, (3) Ex-N-GNSs) and (4) composite **1** as cathode in oxygen atmosphere.

The electrochemical performance of GNSs, N-GNSs, Ex-N-GNSs, and composite **1** was evaluated as cathodes in lithium-oxygen cell in oxygen atmosphere. Figure 4 shows the first discharge profiles of the lithium-oxygen cells with GNSs, N-GNSs, Ex-N-GNSs, and composite **1** cathodes using discharge current of 0.2 mA at 75 °C. Cell with composite **1** as cathode delivers 4.75 mAh discharge cell capacity. On the other hand, cells composed of GNSs, N-GNSs, and Ex-N-GNSs as cathodes delivered 1.95 mAh, 3.0 mAh and 3.7 mAh discharge capacities, respectively. In comparison to the discharge cell capacity of GNSs, cathode composed of N-GNSs and Ex-N-GNSs demonstrated significantly improved discharge cell capacity. In our previous work on cells composed of carbon blend (mixture of Ketjenblack and Calgon activated carbon) and nitrogen-doped carbon blend under identical conditions delivered 0.7 mAh and 1.44 mAh cell capacity. Thus, cell capacity enhancement is more than two times when the carbon blend is replaced by graphene in the cathode of lithium-oxygen cells; while nitrogen doping in GNSs and exfoliation of nanosheets has further improved the cell capacity by more than two times. Cell based on composite **1** exhibits highest discharge cell capacity among all cathodes studied in this work. This enhancement in cell capacity is due to improved electro-catalytic activity of composite **1** and fast lithium ion transport deep inside the cathode due to superionic conducting LAGP. A gradual decrease in cell discharge from 2.8 to 2.4 V is also observed in Figure 4 for composite **1**. A sharp cell discharge is observed at around 2.1 V for N-GNSs and Ex-N-GNSs; while GNSs show a sharp cell discharge at around 2.5 V. These results are consistent with our previous work wherein, an incremental increase of up to 20 wt% of LAGP in cathode formulation (N-C blend) is reported. It is noticed from Figure 4 that although open circuit voltage (OCV) of all cells are high, there is a significant potential drop during

3

the initial stage of discharge. This potential drop is due to both an activation barrier of cathode chemistry that includes sluggish kinetics, and series resistances between various cell components. Further research work to tailor cathode architecture and improve the cell performance of lithium-oxygen batteries is currently underway.

Conclusion

In conclusion, this work demonstrates excellent cell performance of lithium-oxygen cell with cathode formulation based on GNSs. The discharge cell capacity of the cell with cathode of Ex-N-GNSs with LAGP is 4.75 mAh. This work highlights the importance of novel cathode architecture and opens up a promising approach to develop highly efficient oxygen electrodes for lithium-oxygen cells.

Acknowledgements

References:

1. Van Noorden, R., *Nature,* vol. **507**, pp. 26-28, 2014.

2. Bruce, P.G., S.A. Freunberger, L.J. Hardwick, and J.M. Tarascon, *Nat. Mater.,* vol. **11**, pp. 19-29, 2012.

3. Handbook of Batteries and Fuel Cells, 2nd ed., (Ed: Linden, D.), McGraw-Hill, New York, Chap. 38, 1984.

4. Girishkumar, G., B. McCloskey, A.C. Luntz, SD. Swanson, and W.J. Wilcke, *J. Phys. Chem. Lett.*, vol. **1**, pp. 2193-2203, 2010.

5. Zhang, T., and H.B. Zhou, *Nature Commun.*, DOI: 10.1038/ncomms2855, 2013.

6. Oh, D., J. Qi, Y.C. Lu, Y. Zhang, Y. Shao-Horn, and A.M. Belcher, *Nature Commun,* DOI: 10.1038/ncomms3756, 2013.

7. Lim, H.D., H. Song, J. Kim, H. Gwon, Y. Bae, K.Y. Park, J. Hong, H. Kim, T., Kim, Y.H., Kim, X. Lepro, R. Ovalle-Robles, R.H. Baughman, and K. Kang, *Angew. Chem. Int. Ed., DOI: 10.1002/anie.201400711*, 2014.

8. Abraham, K.M. and Z. Jiang, *J. Electrochem. Soc.,* vol. **143**, pp. 1-5, 1996.

9. Zhang, S.S., D. Foster, and J. Read, *J. Power Sources,* vol. **195**, pp. 1235-1240, 2010.

10. Beattie, S.D., D.M. Manolescu, and S.L. Blair, *J. Electrochem. Soc.,* vol. **156**, pp. A44-A47, 2009.

11. Wang, D., J. Xiao, W. Xu, and J.-G. Zhang, *J. Electrochem. Soc.,* vol. **157**, pp. A760-A764, 2010.

12. Eswaran, M., N. Munichandraiah, and L.G. Scanlon, *Electrochem. Solid State Lett.,* vol. **13**, pp. A121-A124, 2010.

13. Trahey, L., C.S. Johnson, J.T. Vaughey, S.H. Kang, L.J. Hardwick, S.A. Freunberger, P.G. Bruce, and M.M. Thackeray, *Electrochem. Solid State Lett.,* vol. **14**, pp. A64-A66, 2011.

14. Lu, Y.C., Z. Xu, H.A. Gasteiger, S. Chen, K. Hamad-Schifferli, and Y. Shao-Horn, *J. Am. Chem. Soc.,* vol. **132**, pp. 12170-12171, 2010.

15. Ren, X., S.S. Zhang, D.T. Tran, and J. Read, *J. Mater. Chem.,* vol. **21**, pp. 10118-10125, 2011.

16. Laoire, C.O., S. Mukerjee, E.J. Plichta, M.A. Hendrickson, and K.M. Abraham, *J. Electrochem. Soc.,* vol. **158**, pp. 12170-12171, 2010.

17. Freunberger, S.A., Y. Chen, Z. Peng, J.M. Griffin, L.J. Hardwick, F. Barde, P. Novak, and P.G. Bruce, *J. Am. Chem. Soc.,* vol. **133**, pp. 8040-8047, 2011.

18. Meini, S., M. Piana, N. Tsiouvaras, A. Garsuch, and H.A. Gasteiger, *Electrohem. Solid State Lett.,* vol. **15**, pp. A45-A48, 2012.

19. Kim, H., H.D. Lim, J. Kim, and K. Kang, *J.Mater.Chem. A.,* vol. **2**, pp. 33-47, 2014.

20. Yoo, E., J. Nakamura, and H. Zhou, *Energy Environ. Sci.,* vol. **5**, pp. 6928-6932, 2012.

21. Li, Y., J. Wang, X. Li, D. Geng, R. Li, and X. Sun, *Chem. Commun.,* vol. **47,** pp. 9438-9440, 2011.

22. Kumar, B., J. Kumar, R. Leese, J.P. Fellner, S.J. Rodrigues, and K.M. Abraham, *J. Electrochem. Soc.,* vol. **157,** pp. A50-A54, 2010.

23. Kichambare, P., J. Kumar, S. Rodrigues and B. Kumar, *J. Power Sources,* vol. **196**, pp. 3310-3316, 2011.

24. Kichambare, P., S. Rodrigues, and J. Kumar, *ACS Appl. Mater. Interfaces,* vol. **4**, pp. 49-52, 2012.

25. Kichambare, P., and S. Rodrigues, *Energy Technol.,* vol. **1**, pp. 209-211, 2013.